Sliding-mode fuzzy logic controller based direct torque control and ripple minimization of induction motors

S. Sujitha[1], Hima Bindu Eluri[2], P. B. Savitha[3], S. Venkateshwarlu[4]
[1]Department of Electrical and Electronics Engineering, New Horizon College of Engineering, Bengaluru, India
[2]Department of Electrical and Electronics Engineering, Geethanjali College of Engineering and Technology, Hyderabad, India
[3]Department of Electrical and Electronic Engineering, Dayananda Sagar College of Engineering, Bengaluru, India
[4]Department of Electrical and Electronics Engineering, CVR College of Engineering, Hyderabad, India

Article Info

Article history:

Received Dec 9, 2025
Revised Jun 2, 2026
Accepted Aug 19, 2026

Keywords:

Field oriented control
Fuzzy logic controller
Induction motor
MATLAB/Simulink
Sliding mode control

ABSTRACT

Conventional direct torque control is one of the most effective strategies for managing the torque of an induction machine (DTC), which is one of the most common types of machines. Instead, the DTC's inadequate control ability is made worse at low speeds by the audible flux and torque waves that are generated by its extremely low switching frequency. This is because the DTC's switching frequency is exceedingly low. In an effort to address these concerns, a variety of direct torque control strategies focused solely on flux and torque as their primary concerns. An improvement in DTC control and the elimination of ripples in induction motors are the goals of this research, which introduces a sliding mode fuzzy logic controller technique. The complexity of the algorithm, sensitivity of the parameters, the tracking speed, the switching loss, and the ripple reduction properties of the technique will all be thoroughly investigated. Simulation of the control mechanism is performed with MATLAB/Simulink in order to verify that it functions as intended.

Corresponding Author:

Hima Bindu Eluri
Department of Electrical and Electronics Engineering, Geethanjali College of Engineering and Technology
Keesara Mandal, Cheeryal Village, Hyderabad-501303, Telangana, India
Email: himabindu.eee@gcet.edu.in

1. INTRODUCTION

Industrial applications requiring variable speed, low cost, high reliability, and high performance have made extensive use of induction motors. For induction motors, there are several control applications, including flux control and monitoring, speed and torque management, energy optimization, and others [1], [2]. Induction motors (IMs) have a complicated, nonlinear dynamical model [3]. A useful technique that produces high-performance system response and makes it easier to adjust an IM's speed is field-oriented control of an IM [4]. This method's simplification of IM control results in dynamics that are similar to those of a separately excited DC motor [5]. Due to the necessity for feedback from the IM's flow and state variables, this method can also be employed in sensor-less IM control [6], [7]. For the speed management of IM, traditional control systems like PI are combined with field-oriented control techniques [8]. These controllers are sensitive to variations in load and motor parameters because the design of these controllers requires a precise mathematical model of the motor and its accurate parameter values [9], [10]. Variable structure control techniques including sliding mode control (SMC) [11], fuzzy logic-based control [12], neural networks [13], and the combination of fuzzy and neural network control [14], [15] may be utilised to address these issues. When it comes to modelling uncertainties and outside disturbances, SMC is a class of variable structure controllers that has great robustness [16]. The fundamental feature of SMC is that it has a switching control law that enables the stability of the system to be guaranteed [17]. As a result of the switching control law, the system chatters. Methods of fuzzy control are reliable and less model-reliant. They are simple to employ as linguistic rule models [18]. An efficient solution that employs expert knowledge without requiring an understanding of the parameters and structure of the control system is fuzzy sliding mode control [19]. The lack of rigorous design procedures for the fuzzy rules and their membership functions, however, is a significant drawback of this approach [20]. To deal with this challenge, adaptive fuzzy sliding-mode control systems have been presented [21]. For the control of IM based on field-oriented control, a variety of adaptive fuzzy sliding mode control algorithms have been presented in recent years [22]-[24]. These algorithms' adaptation principles were created using Lyapunov stability theory. The nonlinear system is the major application for this approach. It offers the flexible rules needed to automatically adapt to Lyapunov stability conditions.

To take advantage of SMC's capacity to deal with uncertainties, modelling mistakes, external disturbances, and the flexibility and generic function approximation property of fuzzy systems, many recent studies have used the adaptive fuzzy sliding-mode control approach. Moreover, it can be challenging at times to precisely pinpoint the membership function parameters of type-1 fuzzy systems. It is possible to address some ambiguities in the antecedent section and cover a wider variety of membership functions by using type-2 membership functions [25].

This paper's primary innovation is the design of a hybrid sliding-mode fuzzy logic controller (SM-FLC) based direct torque control strategy for induction motor drives, which incorporates fuzzy adaptation into the sliding-mode control scheme to dynamically compensate for torque and flux errors. The goal of the suggested approach is to lessen intrinsic torque and flux ripples, chattering, parameter sensitivity, and subpar low-speed performance of traditional DTC, fixed gain control techniques. For improved torque tracking, decreased electromagnetic torque ripple, improved flux regulation, quick transient response, and increased robustness against load disturbances and motor parameter variations, the suggested controller combines the adaptive nonlinear decision-making capability of fuzzy logic with the robustness of sliding mode control.

In this paper, a new speed controller based on adaptive sliding-mode fuzzy controllers is presented for direct field-oriented control of IM. Given their well-known resistance to noise and parameter changes, adaptive sliding-mode fuzzy controllers would be a better option for dealing with the IM's unknown parameters and changing load. The controller becomes more reliable and efficient through the use of SMC. Fuzzy adaptive sliding controllers. MATLAB/Simulink is used to simulate the suggested approach. The simulation results demonstrate the suggested controller's high-performance ability to control the system. The acquired results are compared with those of existing controllers. When compared to existing controllers, the comparison's findings demonstrate that the suggested technique is more resistant to noise and parameter fluctuations.

There are five sections to this essay: i) Direct field-oriented control of IM and the nonlinear model of IM are introduced in section 2; ii) The adaptive sliding-mode fuzzy controller is discussed in section 3; iii) The simulation setup and results are displayed in section 4. Also, simulation results are contrasted with those of an existing controller; and In section 5, the conclusions are displayed.

2. DIRECT FIELD-ORIENTED CONTROL OF INDUCTION MOTOR

In order to represent a three-phase induction motor in a model, some assumptions are made, such as: A sinusoidal magnetic field (MMF) is produced by distributing the stator windings along the air gap. The number is 16. The rotor has a squirrel-cage shape, and the gap between the two machines stays the same size. In both cases, the coils are identical. We do not account for losses due to saturation of the stator windings, hysteresis, or eddy currents. Both [17] and [18]. The Induction Motor's dynamic behavior in stationary action (α, β) is described below, based on the given.

In the stationary reference (α,β), the stator voltage vector Vs is presented by:

$$V_{s\alpha} = \frac{d\phi_{s\alpha}}{dt} + R_s i_{s\alpha} \quad (1)$$

$$V_{s\beta} = \frac{d\phi_{s\beta}}{dt} + R_s i_{s\beta} \quad (2)$$

$$\overline{V_s} = \frac{d\overline{\phi_s}}{dt} + R_s \overline{\iota_s} \quad (3)$$

The voltage, stator flux, and stator current components in the concordant reference (alpha, beta) are represented by ($V_{s\alpha}$, $V_{s\beta}$), ($\phi_{s\alpha}$, $\phi_{ss\beta}$), (isα, isβ), respectively. The symbol Rs stands for stator resistance. As seen in the Concordance reference (α, β), rotor flow's time derivative is:

$$\frac{d\phi_{\{r\alpha\}}}{dt} = -\mathrm{R}_{\{\mathrm{r}\}} i_{r\alpha} - \omega_{\{\mathrm{m}\}} \Phi_{r\beta} \quad (4)$$

$$\frac{d\phi_{\{r\beta\}}}{dt} = -R_{\{r\}}\, i_{r\beta} - \omega_{\{m\}} \Phi_{r\alpha} \quad (5)$$

($i_{r\alpha}, i_{r\beta}$) represent the current components of the rotor and ($\phi_{r\alpha}$, $\phi_{r\beta}$) represent the flux components of the rotor. The symbols R_r and ω_m stand for rotor resistance and motor speed. Figure 1 represents the control diagram of a sliding-mode fuzzy logic controller-based induction motor.

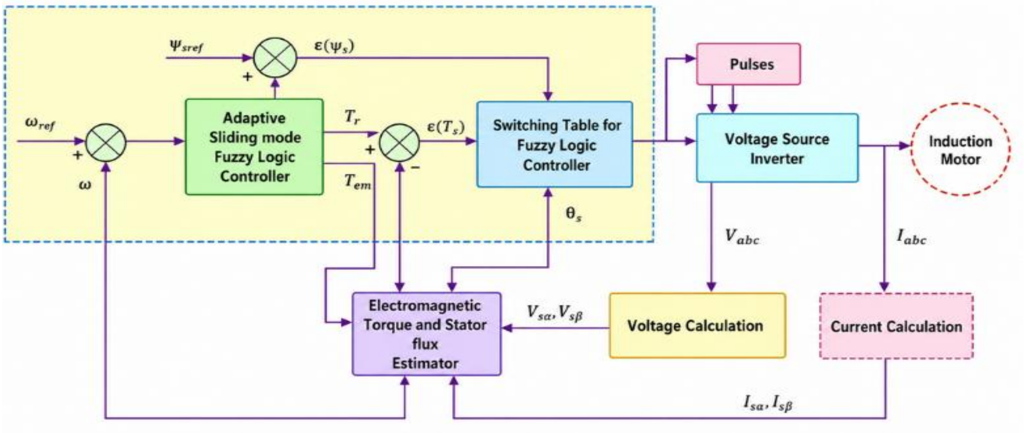

Figure 1. Control diagram of a sliding-mode fuzzy logic controller-based induction motor

One way to express the stator flux vector ϕ_s components is as:

$$\phi_{\{s\alpha\}} = L_{\{s\}i_{\{s\alpha\}}} + \mathrm{M}i_{\{r\alpha\}} \quad (6)$$

$$\phi_{s\beta} = L_s i_{s\beta} + M i_{r\beta} \quad (7)$$

$$\overline{\phi_s} = L_s \overline{\iota_s} + M \overline{\iota_r} \quad (8)$$

One way to express the stator flux vector ϕ_s and its constituents is as:

$$\phi_{r\alpha} = L_r i_{r\alpha} + M i_{s\alpha} \quad (9)$$

$$\phi_{r\beta} = L_r i_{r\beta} + M i_{s\beta} \quad (10)$$

$$\overline{\phi_r} = L_r \overline{\iota_r} + M \overline{\iota_s} \quad (11)$$

Letters L_s, L_r, and M stand for stator, rotor, and mutual inductance, respectively. The following is an abbreviated explanation of how mechanical motors work.

$$J \frac{dohm_m}{dt} = T_{em} - T_l - f ohm_m \quad (12)$$

T_{em} stands for torque, T_l for load torque, J for rotor motion, and f for viscous frictional force. Below is the formula for calculating the electromagnetic torque of the motor.

$$T_{em} = \frac{3}{2} N_p \left(\phi_{s\alpha} i_{s\beta} - \phi_{s\beta} i_{s\alpha} \right) \quad (13)$$

The pole pairs are indicated by N_p. The following figure shows the induction motor's state model, which is defined by the time derivative of stator current and flux components.

$$\frac{di_{s\alpha}}{dt} = -\frac{1}{\sigma}\left(\frac{1}{T_r}+\frac{1}{T_s}\right) i_{s\alpha} - \omega_m i_{s\alpha} + \frac{1}{\sigma L_s T_r}\phi_{s\alpha} + \frac{\omega_m}{\sigma L_s}\phi_{s\beta} + \frac{1}{\alpha L_s} v_{s\alpha} \quad (14)$$

$$\frac{di_{s\beta}}{dt} = -\frac{1}{\sigma}\left(\frac{1}{T_r}+\frac{1}{T_s}\right) i_{s\beta} - \omega_m i_{s\beta} + \frac{1}{\sigma L_s T_r}\phi_{s\beta} + \frac{\omega_m}{\sigma L_s}\phi_{s\alpha} + \frac{1}{\beta L_s} v_{s\beta} \quad (15)$$

$$\frac{d\phi_{s\alpha}}{dt} = v_{s\alpha} + R_s i_{s\alpha} \quad (16)$$

$$\frac{d\phi_{s\beta}}{dt} = v_{s\beta} + R_s i_{s\beta} \quad (17)$$

3. CONTROLLER DESIGN

In an uncertain sliding mode regulator, the fuzzy sliding mode controller is also known as variable structure control. System stability is enhanced by including fuzzy logic control with the standard sliding mode control. No matter how complex or nonlinear the situation, a fuzzy sliding mode controller can handle it. Compared to the original PI controller and the more traditional type 2 fuzzy logic controller, its control response is slower [11]. To ensure the smooth operation of a fuzzy sliding mode controller, it is necessary to design both the sliding surface and the control rule. Eventually, all possible paths through the states of the system will lead to the same point, s = 0. As a result, the sliding surface becomes a desirable flat surface. The control law states that all trajectories have an upper bound on the amount of time they have to reach the sliding manifold, and that once there, they can all stay there forever. After the "Reaching Phase," when the state trajectories go from their beginning states to the sliding manifold, comes the "Sliding Phase," when they stay on the manifold. The phases of reaching and sliding are both dictated by the control law. The process is shown in sliding mode in Figure 2.

$$u(t) = u_{eq} - Msign(s), sign(s) = 1 \quad (18)$$

Anything that produces chattering, an oscillation phenomenon, should be avoided in electrical drives. Their limitations are entirely without merit. Substituting or enhancing the signum function with continuous functions like saturation can reduce this influence. It is possible for a dynamic system to have a thin boundary layer when these functions are continuous. In Figure 3, we can see the chattering effect. Optimizing the control system's performance is as simple as modifying the constant "M" with respect to the amplitude and rate of change of the error signal.

Figure 4 shows the FSMC control architecture. The switching surface is defined by the rotor speed error. Removing the false signal and all of its derivatives is what the control law is all about.

$$e(M) = \omega_{ref}(M) - \omega(M) \quad (19)$$

$$s = \dot{e} + \delta_1 e + \delta_2 \int edt \quad (20)$$

3.1. Mathematical formulation of the sliding-mode fuzzy logic controller

For the induction-motor speed-control system, define the speed tracking error as:

$$e(t) = \omega_m^*(t) - \omega_m(t) \quad (21)$$

where $\omega_m^*(t)$ is the reference rotor speed, and $\omega_m(t)$ is the actual rotor speed. Its derivative is:

$$\dot{e}(t) = \dot{\omega}_m^*(t) - \dot{\omega}_m(t) \quad (22)$$

From the mechanical dynamics of the induction motor given in the manuscript,

$$J\dot{\omega}_m = T_e - T_L - f\omega_m \quad (23)$$

where Te is the electromagnetic torque, TL is the load torque, J is the rotor inertia, and f is the viscous-friction coefficient. Therefore,

$$\dot{e} = \dot{\omega}_m^* - \frac{1}{J}(T_e - T_L - f\omega_m) \quad (24)$$

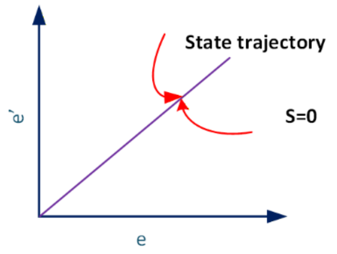

Figure 2. Sliding mode operation

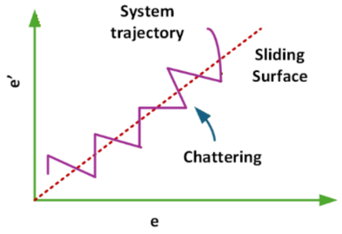

Figure 3. Chattering phenomenon

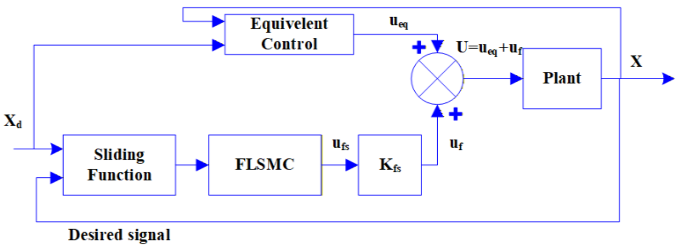

Figure 4. Proposed controller

3.2. Selection and derivation of the sliding surface

Since the objective of the controller is to force the speed error to zero, a first-order sliding surface can be selected as $s = e$ for the speed-control loop. However, to improve transient tracking and explicitly incorporate the error dynamics, a proportional-integral sliding surface can be formulated as (25).

$$s(t) = e(t) \dot{+} \lambda r(t) \tag{25}$$

where λ > 0 is the sliding-surface coefficient. Substituting the speed-error dynamics gives:

$$s = \dot{\omega}_m^* - \frac{T_e - T_L - f\omega_m}{j} + \lambda(\omega_m^* - \omega_m) \tag{26}$$

On the sliding manifold, $s = 0$ and hence $e^{\cdot} + \lambda e = 0$, the resulting error dynamics are:

$$\mathrm{e}(t) = e(0)e,^{-\lambda t} \tag{27}$$

which demonstrates that the tracking error converges exponentially toward zero when λ > 0. Thus, increasing λ generally produces faster error convergence, although excessively large values can increase control effort and sensitivity to measurement noise.

3.3. Sliding-mode control law

The conventional sliding-mode control input can be expressed as (28):

$$u = u_{eq} + u_{sw} \tag{28}$$

where ueq is the equivalent control required to maintain s = 0, while usw is the switching/reaching component. The equivalent control is obtained from the invariance condition $s^{\cdot} = 0$. For the selected surface:

$$\mathrm{s}^{\cdot} = e^{\cdot\cdot} + \lambda e^{\cdot} \tag{29}$$

The switching component is conventionally expressed as (30):

$$usw = -Ksgn(s) \tag{30}$$

where K > 0 is the switching gain. However, the discontinuous sign function produces high-frequency chattering, which is particularly undesirable in electrical drives. The manuscript itself identifies chattering as a major limitation of conventional SMC and suggests replacing the discontinuous switching function with a continuous saturation function.

Therefore, the practical control law can be written as (31):

$$u = u_{eq} - Ksat(\frac{s}{\phi}) \tag{31}$$

where ϕ > 0 defines the boundary-layer thickness:

$$sat(\frac{s}{\phi}) = \begin{cases} 1, & s > \phi \\ \frac{s}{\phi}, & |s| \le \phi \\ -1, & s < -\phi \end{cases} \tag{32}$$

This formulation reduces the chattering associated with the conventional sign function.

3.4. Fuzzy adaptation of the sliding-mode gain

The proposed SM-FLC combines the robustness of sliding-mode control with fuzzy nonlinear decision-making. The manuscript defines the rotor-speed error and its change as the principal variables of the fuzzy controller, with membership functions for error, change in error, and controller output. Accordingly, define:

$$e(k) = \omega_m^*(k) - \omega_m(k) \tag{33}$$

and

$$\Delta e(k) = e(k) - e(k-1) \tag{34}$$

The fuzzy controller generates an adaptive correction/gain:

$$K_f = F[e, \Delta e] \tag{35}$$

where F(·) represents the fuzzy inference mechanism. The SM-FLC control law can consequently be expressed as (36):

$$u = u_{eq} - K_f(e, \Delta e)\ sat\,\frac{s}{\phi} \tag{36}$$

where Kf(e, Δe) > 0 is adjusted according to the instantaneous tracking error and its rate of change. For large errors, the fuzzy controller can generate a larger control action to accelerate convergence. As the trajectory approaches the sliding surface, the fuzzy output is reduced, thereby decreasing oscillations and control effort.

3.5. Lyapunov stability condition

To establish stability, select the Lyapunov candidate function:

$$V = \frac{1}{2}s^2 \tag{37}$$

which satisfies V > 0, $s \neq 0$. Its time derivative is $V^{\cdot} = ss^{\cdot}$. For asymptotic stability, the reaching condition must satisfy $ss^{\cdot} < 0$ for s≠0. For the ideal switching controller, suppose:

$$s^{\cdot} = d(t) - Kfsgn(s) \tag{38}$$

where d(t) represents the lumped uncertainty and disturbance and is bounded by (39).

$$\mid d(t) \mid \le dmax. \tag{39}$$

Then:

$$V^{\cdot} = s[d(t) - Kfsgn(s)] \tag{40}$$

Since ssgn(s)=|s|, we obtain:

$$V^{\cdot} = sd(t) - Kf \mid s \tag{41}$$

using:

$$sd(t) \leq | s | dmax \quad (42)$$

gives:

$$V^{\cdot} \leq -(Kf - dmax) | s | \quad (43)$$

Therefore, the sufficient stability condition is:

$$Kfdmax > 0 \quad (44)$$

which guarantee $V^{\cdot} < 0, s \neq 0.$ Hence, the system trajectories are driven toward the sliding surface and the speed-tracking error converges toward zero.

3.6. Fuzzy stability constraint

Because Kf is generated adaptively by the fuzzy controller, the fuzzy output should be constrained such that:

$$Kf(e, \Delta e) > dmax + \eta \quad (45)$$

where $\eta > 0$ is a positive robustness margin. This condition is important because the fuzzy adaptation should not violate the fundamental SMC stability requirement. The fuzzy logic changes the magnitude of the control action, while the sliding-mode structure gives robustness to bounded uncertainties and load disturbances. The speed tracking error is defined as $e = \omega_m^* - \omega_m$, where ω_m^* is the reference rotor speed, and ω_m is the actual rotor speed. To ensure rapid convergence of the speed error, the sliding surface is chosen as $s = e\dot{+}\lambda e$ where $\lambda > 0$ is the convergence rate. On the sliding manifold s = 0, the error dynamics become $e^{\cdot} + \lambda e = 0$, yielding $e(t) = e(0)e - \lambda t$, which confirms exponential convergence of the tracking error. The control input consists of an equivalent component and an adaptive switching component, $u = u_{eq} - K_f sat(s/\phi)$, where K_f is generated by the fuzzy controller using the speed error and its change as inputs. The saturation function is employed instead of the discontinuous sign function to reduce chattering. For stability analysis, the Lyapunov function $V=1/2s^2$ is selected. Its derivative is $\dot{V}$ = ss. Considering a bounded lumped disturbance $|d(t)|\leq d_{max}$, the switching dynamics satisfy $V\leq-(K_f-d_{max})|s|$. Therefore, selecting the fuzzy-adapted switching gain such that $K_f > d_{max} > 0$ guarantees $V < 0$, satisfying the reaching condition $ss < 0$. Consequently, the system trajectories converge toward the sliding manifold and the speed tracking error approaches zero. This formulation illustrates that the fuzzy adaptation enhances transient response and maintains the robustness and stability properties of the sliding mode control. Figure 5 and Figure 6 indicate modifications in the membership function in error or change in error, respectively, and Figure 7 shows the membership function of the output.

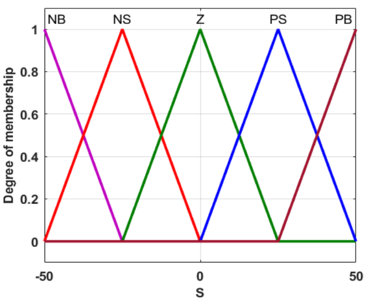

Figure 5. Membership function for error

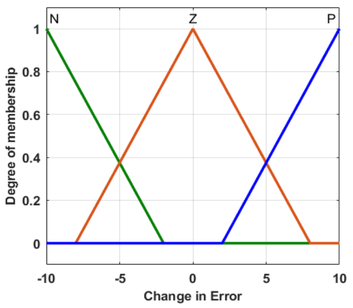

Figure 6. Membership function for change in error

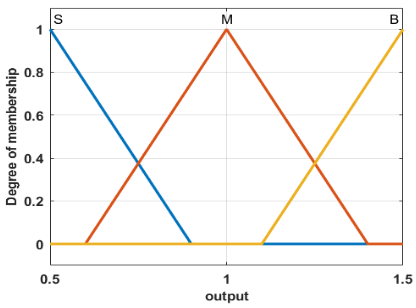

Figure 7. Membership function for output

4. RESULTS AND DISCUSSION

Dynamic modeling and simulation of a three-phase induction motor was performed using MATLAB/Simulink. Induction motor power ratings, low and high, were used to test the model. Additionally, it tested under three different load scenarios: no load, constant load, and variable load. The outcomes are examined in the instances that follow.

4.1. At no load conditions

Traditional PI and FLSMC speed and torque metrics are displayed in Figure 8 and Figure 9, respectively. It seems that the rising time decreases when the sliding-mode fuzzy logic controller (SMFLC) is included in the simulation model and both findings are collected simultaneously. PI's rise time is 0.3435 seconds, whereas SMFLC's is 0.3350 seconds. The graph doesn't show a little change in Tr, M(overshoot), and Ts. Figure 10 demonstrates the variation of IM's torque and speed characteristics for all controllers.

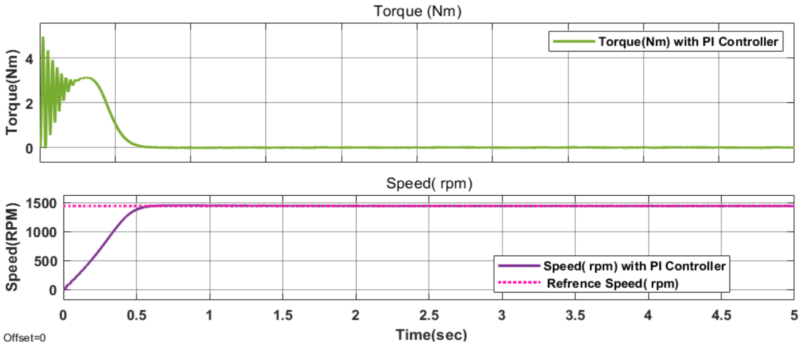

Figure 8. Torque and speed characteristics of PI controller

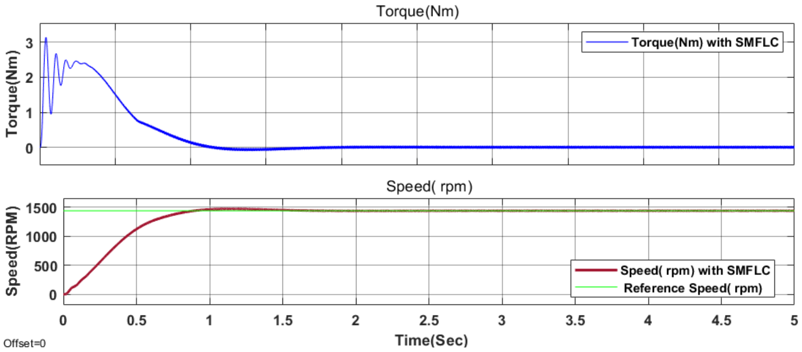

Figure 9. Torque and speed characteristics of SMFLC controller

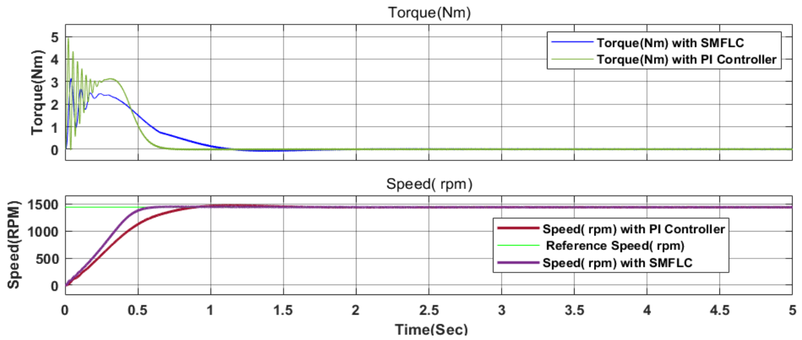

Figure 10. Torque and Speed characteristics of IM using PI and SMFLC controllers

4.2. At constant load

Figure 11 displays the torque parameters for PI, while Figure 12 shows the speed parameters for SMFLC. When a 14 Nm load is applied quickly at 2 seconds, both torque and speed decrease. At 1.9466 seconds with the SMFL controller and 1.8787 seconds with the PI controller, the motor settles after the initial transient. Tuning the PI controller at rated conditions allows for a fair comparison. Figure 10 displays the simulated outcomes for a motor started with a constant load of 4.5 Nm. How well the drive works in contrast to more conventional drive systems that rely on PI and SMFLC. The PI controller is slower to get up to speed than the fuzzy controller when a constant load is suddenly added. In Figure 13, we can see how the torque and speed characteristics of the IM vary for each controller.

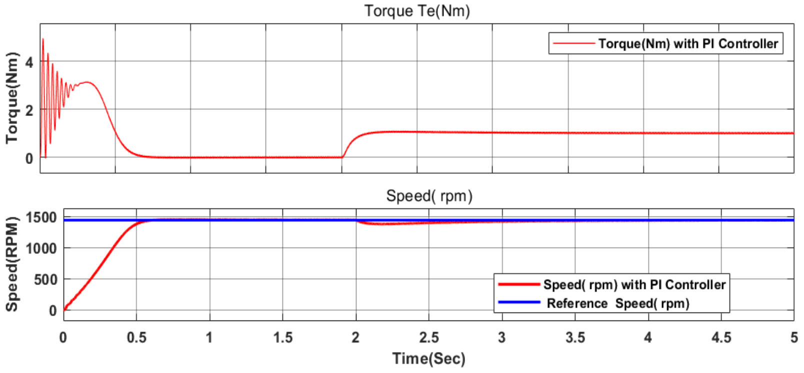

Figure 11. Torque and speed characteristics of the PI controller

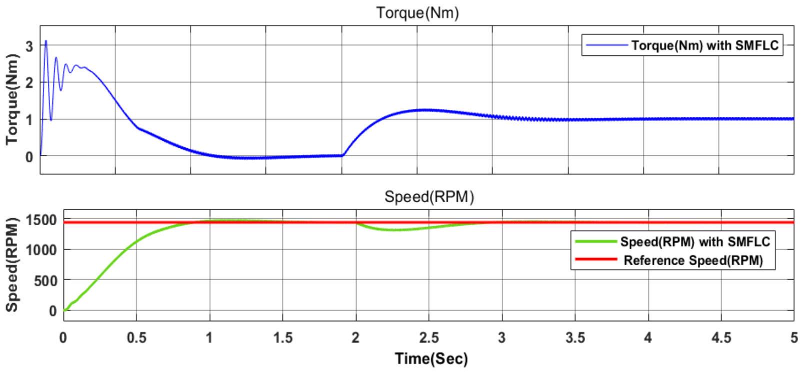

Figure 12. Torque and speed characteristics of SMFLC controller

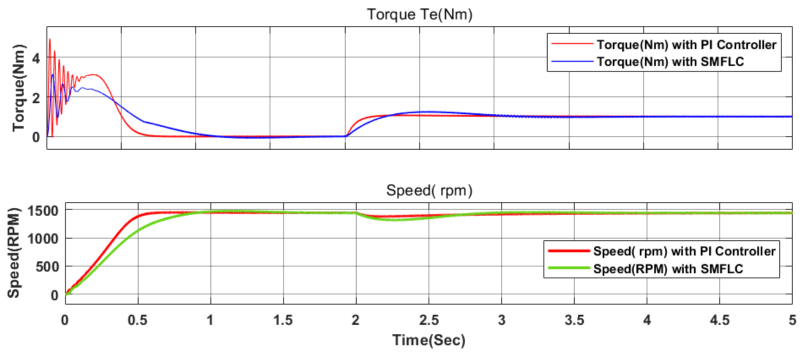

Figure 13. Torque and speed characteristics of IM using PI and SMFLC controllers

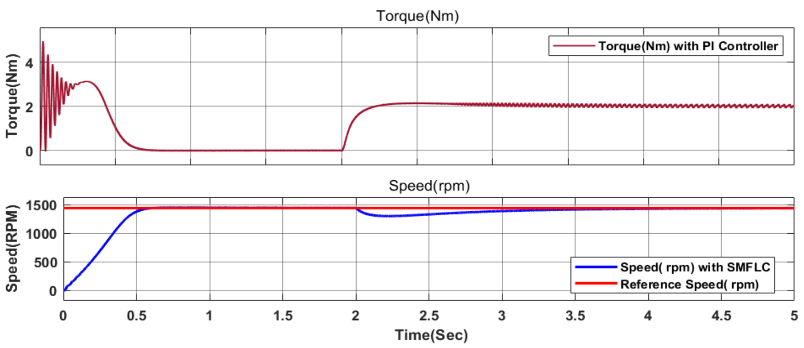

Figure 14. Torque and speed characteristics of PI controller

4.3. At variable load

Figure 15 shows that the speed response is quick and seamless when employing an SMFL controller, in contrast to a PI controller, which has a peak at 0.6 seconds. With an SMFL controller, the motor speed reacts quickly and has 0% steady-state error; it follows its reference. However, when the starting current is high, the PI controller shows steady-state inaccuracy. Keep in mind that the speed response is affected by the load conditions. This is a drawback of a PI controller when the operating conditions are subject to change. Its steady-state error and rise-time metrics are better met by the SMFL controller. Figure 16 demonstrates the variation of IM's torque and speed characteristics for all controllers.

Table 1 shows the parameter specification of the proposed work. For different load situations, Table 2 compares the performance of the PI and SMFLCC controllers in steady-state and transient operation with respect to Tr, M(overshoot), and Ts. Under different load conditions, FLSMC outperforms PI in terms of rise time, settling time, and overshoot, as shown in the tables. This causes the FLSMC controller to surpass the PI controller in performance. That the three-phase induction motor can respond quickly and precisely without overshoot or steady-state inaccuracy is demonstrated here. The results are showing speed and torque charcteristics with different controllers like PI which are depicted in Figure 14.

Table 1. Simulation parameters of the proposed SMFLC-based induction motor drive

Category	Parameter	Symbol	Value
Induction motor	Rated power	(P_n)	4 kW
	Rated line voltage	(Vn)	415 V
	Rated frequency	(f_n)	50 Hz
	Number of phases	—	3
	Number of poles	(P)	4
	Rated speed	(N_r)	1440 rpm
	Stator resistance	(R_s)	1.405 Ω
	Rotor resistance	(R_r)	1.395 Ω
	Stator leakage inductance	(L_{ls})	5.839 mH
	Rotor leakage inductance	(L_{lr})	5.839 mH
	Mutual inductance	(L_m)	172.2 mH
	Stator self-inductance	(L_s)	178.039 mH
	Rotor self-inductance	(L_r)	178.039 mH
	Rotor inertia	(J)	0.0131 kg·m²
	Friction coefficient	(B)	0.002985 N·m·s/rad
Inverter	Topology	—	Three-phase VSI
	DC-link voltage	(V_{dc})	600 V
	Switching frequency	(f_{sw})	10 kHz
	Modulation technique	—	SVPWM
	Semiconductor devices	—	IGBT/Diode
Simulation	Software	—	MATLAB/Simulink
	Simulation duration	(T_{sim})	4 s
	Solver/sample time	(T_s)	(1\times10^{-6}) s
	Controller sampling period	(T_c)	(1\times10^{-4}) s
SMFLC	Speed-error input	(e)	(\omega^*-\omega)
	Change in error	(Δe)	(e(k)-e(k-1))
	Sliding surface coefficient	(λ)	50
	Switching gain	(K)	20
	Boundary-layer thickness	(ϕ)	0.01
	Error scaling factor	(K_e)	1
	Change-error scaling factor	$(K_{\Delta e})$	0.1
	Output scaling factor	(K_u)	1
	Number of fuzzy inputs	—	2
	Number of fuzzy outputs	—	1
	Membership functions/input	—	7
	Membership functions/output	—	7
	Defuzzification	—	Centroid
Load conditions	No-load condition	(T_L)	0 N·m
	Initial/constant load	(T_L)	4.5 N·m

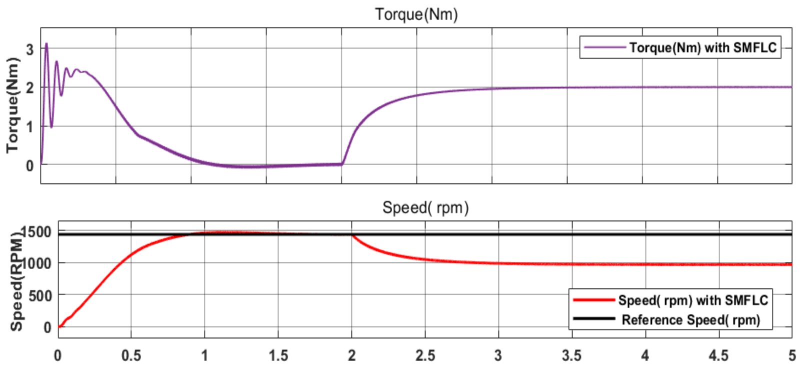

Figure 15. Torque and speed characteristics of IM with SMFLC

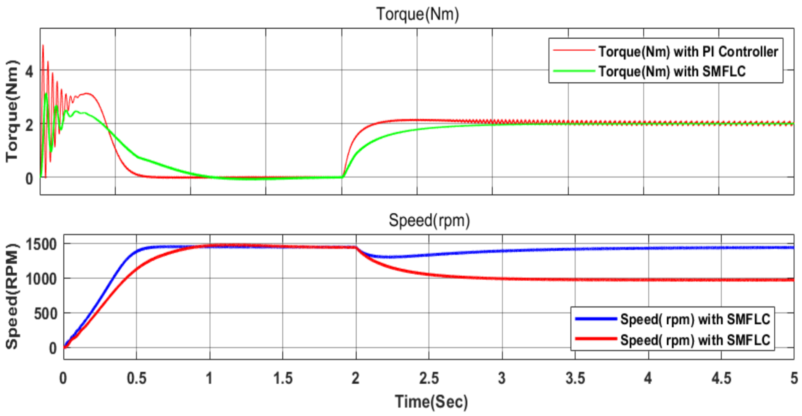

Figure 16. Torque and speed characteristics of IM using PI and SMFLCs

Table 2. Dynamic performance comparison between PI and FOFLC during transient operation

Controller	Rise time (s)	Improvement in rise time (%)	Overshoot (%)	Reduction in overshoot (%)	Settling time (s)	Reduction in settling time (%)
PI	0.5516	10.21	0.6290	3.25	1.9466	2.56
FLC	0.4825	12.53	0.5987	4.82	1.8787	3.49
FOPI	0.2873	47.91	0.4564	27.44	1.7641	9.35
FOFL	0.2641	52.12	0.4064	35.39	1.6423	15.63
FLSMC (Proposed)	0.2114	61.68	0.3218	48.84	1.3025	33.09

5. CONCLUSION

The proposed SMFLC was developed to improve the dynamic performance and robustness of a three-phase induction-motor drive under different operating conditions. MATLAB/Simulink simulations were performed under no-load, constant-load, and variable-load conditions. The quantitative results demonstrate that the proposed FLSMC provides superior transient performance compared with the conventional PI controller. The rise time was improved by 61.68% from 0.5516 s to 0.2114 s. The maximum overshoot was reduced from 0.6290% to 0.3218% (48.84% reduction in overshoot), and the settling time was reduced from 1.9466 s to 1.3025 s (33.09% reduction in settling time). The investigated controllers were PI, FLC, FOPI, FOFL, and FLSMC. The FLSMC controller has given the lowest rise time, overshoot, and settling time. The proposed controller has shown efficient speed control under variable load conditions with 0% steady-state speed error in variable load operation. In the future, we will concentrate on the experimental verification using a laboratory induction-motor drive and the real-time implementation on DSP or FPGA platforms. Other quantitative tests will include speed reversal of ±1500 rpm, low-speed operation of 300 rpm, low-speed reversal, and severe load disturbances. The proposed SMFLC will also be compared with predictive DTC, adaptive DTC, and intelligent DTC by using torque ripple, speed error, settling time, switching losses, and computational time as evaluation metrics. In addition, we will consider the optimization-based tuning of fuzzy membership functions and sliding-mode gains to further reduce the torque ripple, transient time, and computational burden, while maintaining robust operation under parameter variations and disturbances.

FUNDING INFORMATION

Authors state no funding involved.

AUTHOR CONTRIBUTIONS STATEMENT

This journal uses the Contributor Roles Taxonomy (CRediT) to recognize individual author contributions, reduce authorship disputes, and facilitate collaboration.

Name of Author	C	M	So	Va	Fo	I	R	D	O	E	Vi	Su	P	Fu
S. Sujitha	✓	✓	✓	✓	✓	✓			✓	✓			✓	
Hima Bindu Eluri		✓	✓			✓		✓	✓	✓	✓	✓		
P. B. Savitha	✓			✓		✓	✓			✓	✓		✓	
S. Venkateshwarlu					✓		✓			✓		✓		

C : **C**onceptualization
M : **M**ethodology
So : **So**ftware
Va : **Va**lidation
Fo : **Fo**rmal analysis
I : **I**nvestigation
R : **R**esources
D : **D**ata Curation
O : Writing - **O**riginal Draft
E : Writing - Review & **E**diting
Vi : **Vi**sualization
Su : **Su**pervision
P : **P**roject administration
Fu : **Fu**nding acquisition

CONFLICT OF INTEREST STATEMENT

Authors state no conflict of interest.

DATA AVAILABILITY

The data supporting the findings of this study are available from the corresponding author, [HBE], upon reasonable request. However, the data are not publicly available because they contain information that may compromise the privacy of research participants.

REFERENCES

[1] I. Takahashi and T. Noguchi, “Take a look back upon the past decade of direct torque control [of induction motors],” in *Proceedings of the IECON’97 23rd International Conference on Industrial Electronics, Control, and Instrumentation (Cat. No.97CH36066)*, vol. 2, pp. 546–551, doi: 10.1109/IECON.1997.671792.

[2] E. Himabindu, D. Krishna, and V. M. Gopala, “Performance of intelligent controller-based bearingless switched reluctance motor,” *Lecture Notes in Electrical Engineering*, vol. 767, pp. 355–373, 2022, doi: 10.1007/978-981-16-1642-6_28.

[3] J. Zhao and B. K. Bose, “Evaluation of membership functions for fuzzy logic controlled induction motor drive,” in *IEEE 2002 28th Annual Conference of the Industrial Electronics Society. IECON 02*, vol. 1, pp. 229–234, doi: 10.1109/IECON.2002.1187512.

[4] M. Adamczyk and T. Orlowska-Kowalska, “Postfault direct field-oriented control of induction motor drive using adaptive virtual current sensor,” *IEEE Transactions on Industrial Electronics*, vol. 69, no. 4, pp. 3418–3427, Apr. 2022, doi: 10.1109/TIE.2021.3075863.

[5] Y. Zahraoui, M. Akherraz, and S. Elbadaoui, “Fuzzy logic speed control and adaptation mechanism-based twelve sectors DTC to improve the performance of a sensorless induction motor drive,” *International Journal on Electrical Engineering and Informatics*, vol. 13, no. 3, pp. 508–529, Sep. 2021, doi: 10.15676/ijeei.2021.13.3.1.

[6] Z. Farooq, A. Rahman, and S. A. Lone, “System dynamics and control of EV incorporated deregulated power system using MBO-optimized cascaded ID-PD controller,” *International Transactions on Electrical Energy Systems*, vol. 31, no. 11, Nov. 2021, doi: 10.1002/2050-7038.13100.

[7] F. Aymen, N. Mohamed, S. Chayma, C. H. R. Reddy, M. M. Alharthi, and S. S. M. Ghoneim, “An improved direct torque control topology of a double stator machine using the fuzzy logic controller,” *IEEE Access*, vol. 9, pp. 126400–126413, 2021, doi: 10.1109/ACCESS.2021.3110477.

[8] B. Singh, R. Kumar, and P. Kant, “Adjustable speed induction motor drive fed by 13-level cascaded inverter and 54-pulse converter,” *IEEE Transactions on Industry Applications*, vol. 58, no. 1, pp. 890–900, 2022, doi: 10.1109/TIA.2021.3127855.

[9] S. A. A. Tarusan, A. Jidin, and M. L. M. Jamil, “The optimization of torque ripple reduction by using DTC-multilevel inverter,” *ISA Transactions*, vol. 121, pp. 365–379, Feb. 2022, doi: 10.1016/j.isatra.2021.04.005.

[10] C. P. Gor, V. A. Shah, and B. Rangachar, “Fuzzy logic based dynamic performance enhancement of five phase induction motor under arbitrary open phase fault for electric vehicle,” *International Journal of Emerging Electric Power Systems*, vol. 22, no. 4, pp. 473–492, Aug. 2021, doi: 10.1515/ijeeps-2020-0271.
[11] S. R. Satpathy, S. Pradhan, R. Pradhan, R. Sahu, A. P. Biswal, and B. P. Ganthia, “Direct torque control of mathematically modeled induction motor drive using pi-type-i fuzzy logic controller and sliding mode controller,” *Lecture Notes in Networks and Systems*, vol. 185 LNNS, pp. 239–251, 2021, doi: 10.1007/978-981-33-6081-5_21.
[12] I. Eke, M. Saka, H. Gozde, Y. Arya, and M. C. Taplamacioglu, “Heuristic optimization based dynamic weighted state feedback approach for 2DOF PI-controller in automatic voltage regulator,” *Engineering Science and Technology, an International Journal*, vol. 24, no. 4, pp. 899–910, Aug. 2021, doi: 10.1016/j.jestch.2020.12.023.
[13] B. P. Ganthia, R. Pradhan, R. Sahu, and A. K. Pati, “Artificial ant colony optimized direct torque control of mathematically modeled induction motor drive using PI and sliding mode controller,” *Lecture Notes in Electrical Engineering*, vol. 707, pp. 389–408, 2021, doi: 10.1007/978-981-15-8586-9_35.
[14] Z. Wang, W. Sun, and D. Jiang, “Stability analysis and trajectory design of a nonlinear switching system for speed sensorless induction motor drive,” *IEEE Transactions on Industrial Electronics*, vol. 69, no. 6, pp. 5514–5524, Jun. 2022, doi: 10.1109/TIE.2021.3086712.
[15] B. Chikondra, U. R. Muduli, and R. K. Behera, “Improved DTC technique for THL-NPC VSI Fed Five-Phase Induction Motor Drive Based on VVs Assessment over a Wide Speed Range,” *IEEE Transactions on Power Electronics*, vol. 37, no. 2, pp. 1972–1981, 2022, doi: 10.1109/TPEL.2021.3102963.
[16] Prince and A. S. Hati, “A comprehensive review of energy-efficiency of ventilation system using Artificial Intelligence,” *Renewable and Sustainable Energy Reviews*, vol. 146, p. 111153, Aug. 2021, doi: 10.1016/j.rser.2021.111153.
[17] J. P. Hoffstaedt *et al.*, “Low-head pumped hydro storage: A review of applicable technologies for design, grid integration, control and modelling,” *Renewable and Sustainable Energy Reviews*, vol. 158, p. 112119, Apr. 2022, doi: 10.1016/j.rser.2022.112119.
[18] I. Osman, D. Xiao, M. Rahman, M. Norambuena, and J. Rodriguez, “An optimal reduced-control-set model predictive flux control for 3L-NPC fed induction motor drive,” *IEEE Transactions on Energy Conversion*, vol. 36, no. 4, pp. 2967–2976, Dec. 2021, doi: 10.1109/TEC.2021.3065373.
[19] D. Krishna, M. Sasikala, and V. Ganesh, “Mathematical modeling and simulation of UPQC in distributed power systems,” in *2017 IEEE International Conference on Electrical, Instrumentation and Communication Engineering (ICEICE)*, Apr. 2017, pp. 1–5. doi: 10.1109/ICEICE.2017.8191886.
[20] D. Krishna, M. Sasikala, and R. Kiranmayi, “FOPI and FOFL controller based UPQC for mitigation of power quality problems in distribution power system,” *Journal of Electrical Engineering & Technology*, vol. 17, no. 3, pp. 1543–1554, May 2022, doi: 10.1007/s42835-022-00996-6.
[21] D. Krishna, M. Sasikala, and V. Ganesh, “Adaptive FLC-based UPQC in distribution power systems for power quality problems,” *International Journal of Ambient Energy*, vol. 43, no. 1, pp. 1719–1729, Dec. 2022, doi: 10.1080/01430750.2020.1722232.
[22] S. Krim, Y. Krim, and M. F. Mimouni, “Sensorless direct torque control based on nonlinear integral sliding mode controllers for an induction motor drive: Experimental verification,” *Proceedings of the Institution of Mechanical Engineers, Part I: Journal of Systems and Control Engineering*, vol. 235, no. 2, pp. 249–268, Feb. 2021, doi: 10.1177/0959651820933733.
[23] S. Mahfoud, A. Derouich, N. E. Ouanjli, M. E. Mahfoud, and M. Taoussi, “A New strategy-based PID controller optimized by genetic algorithm for DTC of the doubly fed induction motor,” *Systems*, vol. 9, no. 2, p. 37, May 2021, doi: 10.3390/systems9020037.
[24] D. Krishna, M. Sasikala, and V. Ganesh, “Fractional order PI based UPQC for improvement of power quality in distribution power system,” *International Journal of Innovative Technology and Exploring Engineering*, vol. 8, no. 7, pp. 322–327, 2019.
[25] A. Mohan, M. Khalid, and A. C. Binojkumar, “Performance analysis of permanent magnet synchronous motor under DTC and space vector-based DTC schemes with MTPA control,” in *2021 International Conference on Communication, Control and Information Sciences (ICCISc)*, Jun. 2021, pp. 1–8, doi: 10.1109/ICCISc52257.2021.9484869.

BIOGRAPHIES OF AUTHORS

S. Sujitha completed her Ph.D. in electrical engineering from Anna University in 2016. She has 20 years of teaching experience in electrical and electronics engineering for undergraduate and postgraduate students, as well as 12 years of research and administrative experience. She is currently working as a professor at New Horizon College of Engineering, Bengaluru, and also serves as a research supervisor at Visvesvaraya Technological University, Karnataka. Her research interests include digital systems, embedded systems, EV automation, artificial intelligence, data analytics, VLSI, renewable energy, smart grids, and soft computing. She has published papers in several international journals and conferences. She is a life member of ISTE and IEEE and has chaired sessions at various international conferences. She has received and completed 18 research grants from various government funding agencies, such as AICTE AQIS, VGST, KSCST, and VTU. She received the “Outstanding Young Engineer Award” and “Best Performing Professor” Award from ITCA and the Committee for Space Programme Development, Serbia, during Indo-Serbia Engineers Day on September 15, 2021. She also received a “Certificate of Award” from the UNITYsat Team for her contribution to the successful design, development, fabrication, integration, testing, launch, and operation of UNITYsat on February 28, 2021, at SDSC-SHAR, Sriharikota, from UNISEC India. She can be contacted at email: dr.s.sujitha@gmail.com.

Hima Bindu Eluri is an associate professor in the Department of Electrical and Electronics Engineering at Geethanjali College of Engineering and Technology, Hyderabad, with 18 years of teaching experience. She received her Ph.D. in renewable energy and energy management from Andhra University, her M.Tech. from Jawaharlal Nehru Technological University (JNTU), Hyderabad, and her B.Tech. from Bapatla Engineering College. She has published more than 25 research papers in international journals and conference proceedings. She serves as a Faculty Advisor for the IEEE Power & Energy Society and is also a senior member of IEEE. Her research interests include power quality, microgrids, and renewable energy sources. She can be contacted at email: himabindu.eee@gcet.edu.in.

P. B. Savitha is currently working as an associate professor in the Department of Electrical and Electronics Engineering at DSCE, Bengaluru, with 25 years of teaching experience. She completed her B.E. in electrical and electronics engineering from the University of Mysore, her M.Tech in digital communication from Uttar Pradesh Technical University, and her Ph.D. in electrical and electronics engineering from Visvesvaraya Technological University (VTU), Belagavi, in 2018. Her research interests include solar photovoltaic systems, power quality issues in renewable energy integration, power electronic converters for renewable energy integration, machine learning, and power electronic converters for electric vehicles. She has published papers in several international journals and conferences. She is a life member of ISTE and IEEE and has chaired sessions at various international conferences. She has also executed funded projects under the AICTE MODROB scheme. She can be contacted at email: savithapb-eee@dayanandasagar.edu.

S. Venkateshwarlu completed his M.Tech. from NIT Warangal and his Ph.D. in electrical engineering from Osmania University, Hyderabad, in 2011. He has 30 years of teaching experience in electrical and electronics engineering for undergraduate and postgraduate students, along with 14 years of research and administrative experience. He served as an Indian expatriate teacher at Arba Minch University, Ethiopia, Africa, for three years from 2004 to 2007. He is currently working as a professor at CVR College of Engineering, Hyderabad. In addition to teaching, he serves as a research supervisor at JNTUH and JNTUK. Two scholars have completed their Ph.D., and one scholar is due to submit their Ph.D. thesis under his guidance. He served as the Head of the Department of Electrical and Electronics Engineering at CVRCE for 10 years and has been serving as the Controller of Examinations at CVRCE since May 2025. His research interests include power electronics, wind energy, electric and hybrid vehicles, and smart grids. He has published more than 50 papers in international journals and conferences. He can be contacted at email: svip123@gmail.com.